Cavity-enhanced optical bottle beam as a mechanical amplifier

Tim Freegarde*
Dipartimento di Fisica, Università di Trento, Via Sommarive 14, 38050 Povo-Trento (TN), Italy

Kishan Dholakia
J. F. Allen Physics Research Laboratories, School of Physics and Astronomy, University of St. Andrews, North Haugh, St. Andrews, Fife KY16 9SS, Scotland

(Received 22 March 2002; published 30 July 2002)

We analyze the resonant cavity enhancement of a hollow ''optical bottle beam'' for the dipole-force trapping of dark-field-seeking species. We first improve upon the basic bottle beam by adding further Laguerre-Gaussian components to deepen the confining potential. Each of these components itself corresponds to a superposition of transverse cavity modes, which are then enhanced simultaneously in a confocal cavity to produce a deep optical trap needing only a modest incident power. The response of the trapping field to displacement of the cavity mirrors offers an unusual form of mechanical amplifier in which the Gouy phase shift produces an optical Vernier scale between the Laguerre-Gaussian beam components.

DOI: 10.1103/PhysRevA.66.013413 PACS number(s): 42.50.Vk, 32.80.Pj, 42.60.Da, 42.60.Jf

I. INTRODUCTION

The dipole force [1] provides an optical means of trapping and guiding atoms and molecules without relying upon the disturbing process of spontaneous emission, which can heat the species and cause loss of population from the trapped states, or introducing the sensitivity to quantum state that is characteristic of traps based upon magnetic fields. Residual scattering can be reduced by detuning the optical field far from resonance with the radiative transition [2,3], but the intensity must be raised for the strength of the force to be maintained.

Depending upon whether the optical field is detuned to the red or the blue of the radiative transition, the dipole force can act towards or away from regions of high intensity. In most applications, the laser has been detuned to the red, so that atoms are attracted towards the intense focus of the laser beam [4] and, despite some residual scattering, such schemes have been used to produce [5] and transport [6] Bose-Einstein condensates, control the delivery of single atoms [7], and trap caesium dimers [8]. If the laser is instead detuned to the blue of the transition, the species seek dark, low-field regions where they are substantially undisturbed and storage times can approach the order of a second [9]. Rather than zones of high intensity, such as the focus of a Gaussian laser beam, blue-detuned traps require regions of low intensity that are completely surrounded by a brighter optical field. Such fields are not offered by a simple TEM_{00} laser mode, and various schemes have instead been adopted, using sheets of light [10], the time average of a mechanically rotated laser beam [11], cylindrical optics [12,13], wave plates [9,14], axicon lenses [15–17], and more robustly, holographic mode converters [18,19].

Since optical absorption by the confined species is usually tiny, resonant cavities offer an attractive means of enhancing the radiation field of a low-power laser [20–22]. It is not, however, only the TEM_{00} cavity modes that are unsuitable for providing a blue-detuned trapping field: so, too, are the individual higher-order modes of a standing-wave cavity, for the exact cancellation of the forward and backward traveling beams produces nodal surfaces of zero intensity along which dark-field-seeking species would escape. Even the Laguerre-Gaussian modes of a traveling wave cavity, which have been used for trapping in two dimensions [19,23–25], cannot provide axial confinement, which requires additional beams [12].

Optical fields suitable for the confinement of dark-field-seeking species must therefore be superpositions of cavity modes, and some proposed geometries have indeed been analyzed as such [19,26]. For such fields to be enhanced by an optical cavity, the component modes must naturally be resonant simultaneously, and we therefore require the cavity to be confocal and the trapping field to have a definite symmetry. It is also important that interference from the returning beam that the cavity generates should not produce the same nodal surfaces as occur for individual cavity modes. We therefore exploit a property of the confocal cavity that images are reproduced only after a complete round trip. This allows the returning beam to differ from the trapping beam, both in detailed structure and in overall scale and hence intensity. In the cavity-mode picture, there are sufficient components for the nodes of the even longitudinal modes to be filled by the antinodes of the odd modes, and vice versa.

In a previous paper [27], we have shown how the cavity enhancement of a single Gaussian beam could produce a coaxial array of dark rings resulting from interference between the unequal forward traveling and returning beams. In this paper, we apply related ideas to an optical bottle beam [9,14,16,17,19], in which coaxial and confocal Laguerre-Gaussian beams of equal azimuthal index but different radial dependence are combined so as to interfere destructively at the center of the focal plane, forming a dark central region that is completely enclosed by a bright trapping layer. Enclosing the Laguerre-Gaussian superposition within a resonant confocal cavity greatly enhances the intensity of the

*Electronic address: tim.freegarde@physics.org

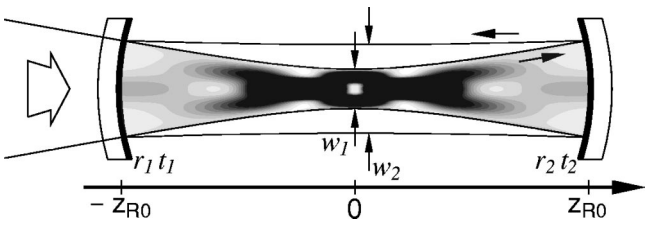

FIG. 1. The confocal cavity can support the complex mode superposition corresponding to an optical bottle beam. Here, the five-component bottle beam is focused into the cavity to form a waist w_1 at the cavity center. The beam is reflected by mirror 2 to form another bottle beam with waist w_2; thanks to its much reduced intensity, this imposes only slight modulation upon the field arising from the forward traveling original. In this figure only, the shading indicates regions of *high* intensity.

trapping field, but its form is modified by the presence of the returning beam. However, by choosing a cavity mode waist that is larger than that of the trapping superposition, we arrange for the reflected beam to be broader and thus much lower in intensity, so that the trapping field is only slightly modified. The arrangement is shown schematically in Fig. 1.

In contrast to our previously considered geometry, formed by interference between the unequal forward traveling and returning beams, the dark trap here results from the interference of copropagating beams. We shall see that this allows an unusual form of mechanical amplification resembling the action of a Vernier scale.

II. OPTICAL BOTTLE BEAMS

Laguerre-Gaussian beams $\mathcal{L}_{pm}$ are paraxial solutions to the wave equation for a focused beam in cylindrical polar coordinates. In essence, they are Gaussian beams $\mathcal{L}_{00}$ that have been modulated transversely so as to introduce p off-axis nodes as a function of radius—and a further axial node for the case $m \neq 0$—and a monotonically increasing azimuthal phase of $2\pi m$ radians per revolution corresponding to the orbital angular momentum of the beam [28]. The electric field of a normalized Laguerre-Gaussian beam of order (p,m), waist radius $w(0)$, and wavelength λ, propagating in a positive direction along the z axis, may be written in terms of the wave number $k=2\pi/\lambda$ and Rayleigh range $z_R = \pi w(0)^2/\lambda$ as

$$\mathcal{L}_{pm}(r,z,\theta) = \sqrt{\frac{4p!}{(1+\delta_{0m})\pi(p+|m|)!}} L_p^{|m|}\left(\frac{2r^2}{w(z)^2}\right) \times \left(\frac{\sqrt{2}r}{w(z)}\right)^{|m|} \frac{\exp[\mathrm{i}(2p+|m|+1)\tan^{-1}(z/z_R)]}{w(z)} \times \exp\left(-\frac{r^2}{w(z)^2} - \frac{\mathrm{i}kr^2}{2R(z)} + \mathrm{i}m\theta - \mathrm{i}kz\right), \quad (1)$$

where $L_p^{|m|}(x)$ is the associated Laguerre polynomial, $R(z) = z + z_R^2/z$, $w(z) = w(0)\sqrt{1+(z/z_R)^2}$, and the origin is at the beam focus. Different orders thus vary differently both with radius and, thanks to the different Gouy phases, with axial position, and it is these properties that allow Laguerre-Gaussian superpositions to form optical bottle beams.

The optical bottle beam may be considered to be a superposition of two or more coaxial and confocal Laguerre-Gaussian beams that are adjusted so as to interfere destructively at the center of the focal plane. At this position, the dissimilar radial dependences of the Laguerre-Gaussian beams cause the exact cancellation to be lost off axis, and the different Gouy phases play a similar role away from the focal plane. This representation was proposed by Arlt and Padgett [19], who used a holographic mode converter to form a simple bottle beam superposition of $\mathcal{L}_{00}$ and $\mathcal{L}_{20}$, the electric field being given by

$$\mathcal{E}^{(2)}(r,z) = \mathcal{L}_{00}(r,z) - \mathcal{L}_{20}(r,z), \quad (2)$$

where the components differ in radial index p by 2 rather than 1 so that the axial intensity maximum occurs at finite z. There is, however, nothing fundamental about this choice of Laguerre-Gaussian components, and alternative combinations may also yield suitable trapping beams—the fields produced using axicon lenses [15–17] being complicated examples—and by adjusting the mode superposition, it is possible to tailor the shape of the trapping field. These modifications add little to the experimental complexity, for such bottle beams are best produced using holographic mode converters designed specifically for the fields required.

Since Laguerre-Gaussian beams with azimuthal index $m \neq 0$ have a node at the beam axis, only those beams with $m=0$ can provide axial confinement. Whilst the dark centers of higher-order modes might make them attractive additions to a bottle beam (noting that only beams with an even difference Δm can be resonant simultaneously), the different azimuthal phases would give the trapping field an angular dependence. In this paper, we restrict ourselves to cylindrically symmetric fields and thus to superpositions of beams for which $m=0$. We further limit our choices to fields that are symmetrical about the focal plane, with the simplifying consequence that the relative amplitudes of the Laguerre-Gaussian components at the trap center must all be real.

For cavity-enhanced fields, there is a further constraint on the superpositions for, as we show in the following section, Laguerre-Gaussian beams acquire a phase of $(-1)^p$ on the half round trip from the waist of the forward traveling beam to that of its reflection. If the field components are to cancel, forming dark centers to both the forward traveling and returning beams, then it follows that the odd-numbered components alone must form a bottle beam, as must those of even radial index. The bottle beam of Arlt and Padgett [19], given in Eq. (2) above, is thus the simplest bottle beam suitable for cavity enhancement.

We have numerically examined some simple beam superpositions with the aim of deepening the bottle by raising the cols (or ''saddle points'') that mark the lowest points of the confining ''wall.'' For the simplest bottle beam of three components, for example, we find the optimum field to have coefficients roughly in the ratio $4:-1:-3$,

$$\mathcal{E}^{(3)}=0.784\mathcal{L}_{00}-0.196\mathcal{L}_{20}-0.589\mathcal{L}_{40}, \tag{3}$$

and the subsequent four-component field to be given by

$$\mathcal{E}^{(4)}=0.772\mathcal{L}_{00}+0.104\mathcal{L}_{20}-0.370\mathcal{L}_{40}-0.506\mathcal{L}_{60}. \tag{4}$$

The traps prove respectively to have col intensities 45% and 87% higher than the two-component arrangement of Eq. (2) with the same laser power and waist radius. However, the trap volumes are in both cases proportionally smaller, and similar fields could be produced simply by focusing the trapping field more tightly.

For the calculations in this paper, we have therefore considered the simplest five-component beam, which combines an even-p bottle beam of three components with an odd-p beam of two,

$$\mathcal{E}^{(5)}=[\mathcal{L}_{00}+x\mathcal{L}_{20}-(1+x)\mathcal{L}_{40}]+y(\mathcal{L}_{10}-\mathcal{L}_{30}). \tag{5}$$

The optimum values of $x=-0.2393$ and $y=0.4804$ give a normalized five-component field,

$$\mathcal{E}^{(5)}=0.6905\mathcal{L}_{00}+0.3317\mathcal{L}_{10}-0.1652\mathcal{L}_{20}-0.3317\mathcal{L}_{30}-0.5252\mathcal{L}_{40}, \tag{6}$$

which has a col intensity over 85% higher than in the two-component case at a radius that is about 20% smaller.

III. CAVITY ENHANCEMENT

Laguerre-Gaussian beams of the form $\mathcal{L}_{pm}(r,z,\theta)$ given in Eq. (1) are the resonant modes of a confocal cavity of length l along the z axis, when $z_R=l/2$ and $z=0$ lies at the center of the cavity. We henceforth label these modes $\mathcal{L}^{(0)}_{pm}$ and the associated waist radius and Rayleigh length $w(0)=w_0$ and $z_R=z_{R0}$, respectively.

A Laguerre-Gaussian beam $\mathcal{L}^{(1)}_{qs}(r,z,\theta)$, whose waist of arbitrary radius w_1 coincides with the waists of the cavity modes with which it is coaxial, may be written as a superposition of the cavity modes

$$\mathcal{L}^{(1)}_{qs}(r,z,\theta)=\sum_{pm} a_{pmq}\mathcal{L}^{(0)}_{pm}(r,z,\theta). \tag{7}$$

where $a_{pmq}=0$ if $m\neq s$. We may write these coefficients for arbitrary p and s and specific values of q (we have not yet succeeded in finding the completely general form), the first five being

$$a_{ps0}=\cos^{s+1}\phi\sqrt{\frac{(p+s)!}{p!s!}}\sin^{p}\phi, \tag{8}$$

$$a_{ps1}=\cos^{s+1}\phi\sqrt{\frac{(p+s)!}{p!(s+1)!}}\sin^{p-1}\phi\,[p\cos^2\phi-(s+1)\sin^2\phi], \tag{9}$$

$$a_{ps2}=\cos^{s+1}\phi\sqrt{\frac{(p+s)!}{2!p!(s+2)!}}\sin^{p-2}\phi\,\{[p\cos^2\phi-(s+1)\sin^2\phi][p\cos^2\phi-(s+2)\sin^2\phi]-p\cos^2\phi\}, \tag{10}$$

$$a_{ps3}=\cos^{s+1}\phi\sqrt{\frac{(p+s)!}{3!p!(s+3)!}}\sin^{p-3}\phi\,(\{[p\cos^2\phi-(s+1)\sin^2\phi][p\cos^2\phi-(s+2)\sin^2\phi][p\cos^2\phi-(s+3)\sin^2\phi]\}$$
$$-3p^2\cos^4\phi+p\cos^2\phi[(3s+5)\sin^2\phi+2]), \tag{11}$$

$$a_{ps4}=\cos^{s+1}\phi\sqrt{\frac{(p+s)!}{4!p!(s+4)!}}\sin^{p-4}\phi\,(\{[p\cos^2\phi-(s+1)\sin^2\phi][p\cos^2\phi-(s+2)\sin^2\phi][p\cos^2\phi-(s+3)\sin^2\phi]$$
$$\times[p\cos^2\phi-(s+4)\sin^2\phi]\}-6p^3\cos^6\phi+p^2\cos^4\phi\,[(12s+26)\sin^2\phi+11]-p\cos^2\phi[(6s^2+26s+26)\sin^4\phi$$
$$+(8s+14)\sin^2\phi+6]), \tag{12}$$

where ϕ depends upon the ratio α of the waist radii of the arbitrary beam w_1 and resonant cavity modes w_0,

$$\alpha=w_0/w_1, \tag{13}$$

$$\sin\phi=\frac{\alpha-\alpha^{-1}}{\alpha+\alpha^{-1}}, \tag{14}$$

$$\cos\phi=\frac{2}{\alpha+\alpha^{-1}}. \tag{15}$$

It is clear that a beam of waist $w_2=\alpha w_0$ (i.e., $\alpha\rightarrow 1/\alpha$, hence $\phi\rightarrow-\phi$) will have the same coefficients a_{psq} apart from a sign-changing term $(-1)^p$. Such a term is indeed introduced with each half round trip of the cavity, as a result of the Gouy phase shift $2\exp[i(2p+|m|+1)\pi/4]$. The cavity mirror thus

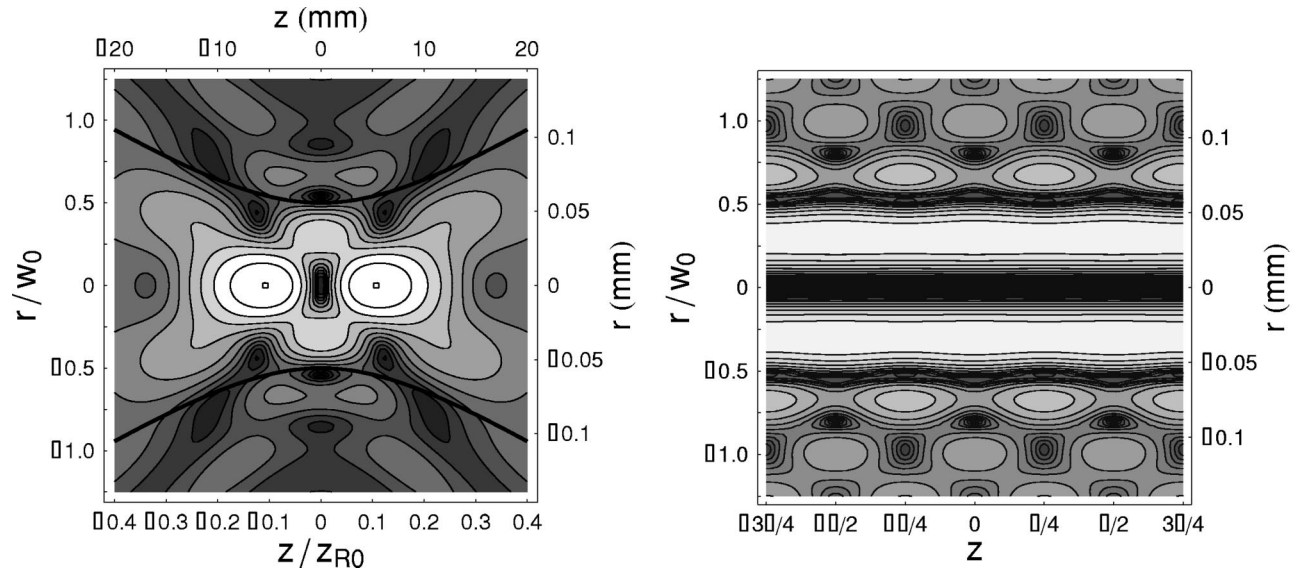

FIG. 2. The intensity distribution within a perfectly confocal resonator. Left: the mean intensity is shown for the central 40% of the cavity. The solid lines show $\pm w_1(z)$, at which the Gaussian beam has fallen to e^{-2} of its intensity on axis. Right: viewed on a wavelength scale around the cavity center, the modulation due to interference between the counterpropagating beams is apparent. Here, $l=100$ mm, $\lambda=780$ nm, and $\alpha=2$. Contours are logarithmic, with four per decade, referred to the peak intensity in the focal plane.

refocuses the Gaussian beam to a waist w_2 at the cavity center, as we would expect from a more conventional treatment of Gaussian beam propagation, and this difference between forward and backward traveling beams destroys the exact cancellation that would prevent confinement. The second cavity mirror causes the original beam to be reproduced after a complete round trip, as each accumulated Gouy phase becomes a whole number of cycles.

There is also a simple form to the Gouy phase acquired by a Laguerre-Gaussian beam $\mathcal{L}_{qs}^{(1)}$ in passing from the waist to the mirror and back, as may be seen by adding the on-axis phases $\phi=-kl/2+(2q+|s|+1)\tan^{-1}(l/2z_R)$ for each half,

$$\begin{aligned}\phi &= -kl+(2q+|s|+1)\{\tan^{-1}(\alpha^2)+\tan^{-1}(\alpha^{-2})\}\\ &= (N+q+|s|/2)\,\pi,\end{aligned} \tag{16}$$

N being the number of axial nodes for the resonant Gaussian beam. Beams of equal s thus incur an additional phase of $(-1)^q$ with each half round trip so that, if an even-q beam and its reflection add constructively in the focal plane, then an odd-q beam will instead see destructive interference (albeit slight, because of the difference in intensity). This is the reason, mentioned in the preceding section, why the superposition $\mathcal{L}_{00}-\mathcal{L}_{10}$, for example, would not form a cavity-enhanced bottle beam, for while the beams cancel in the forward direction, the returning beams add rather than subtract.

For our remaining calculations, we use the five-beam superposition given in Eq. (6). Each of the Laguerre-Gaussian components may be mapped onto cavity modes as in Eq. (7), and the optical field within the ideal confocal cavity may be determined either by using the coefficients a_{p0q} to calculate the cavity mode superposition or by adding the five forward-traveling Laguerre-Gaussian beams to a similar set that return from the cavity mirror with waists $w_2=\alpha w_0$. While the second method is the more straightforward, our subsequent analysis of nonideal cavities will require the first method of analysis.

For this illustration, we consider the trapping of atomic ^{85}Rb, using a 100-mm-long cavity with 99.99% reflecting mirrors to enhance the beam from a 780-nm diode laser, and taking the value $\alpha=2$. With an incident power of 100 mW in the Laguerre-Gaussian beam superposition, giving a circulating power of 1 kW (and hence a trapping intensity around 10 MW cm^{-2} at the col) and an optimal detuning [29]

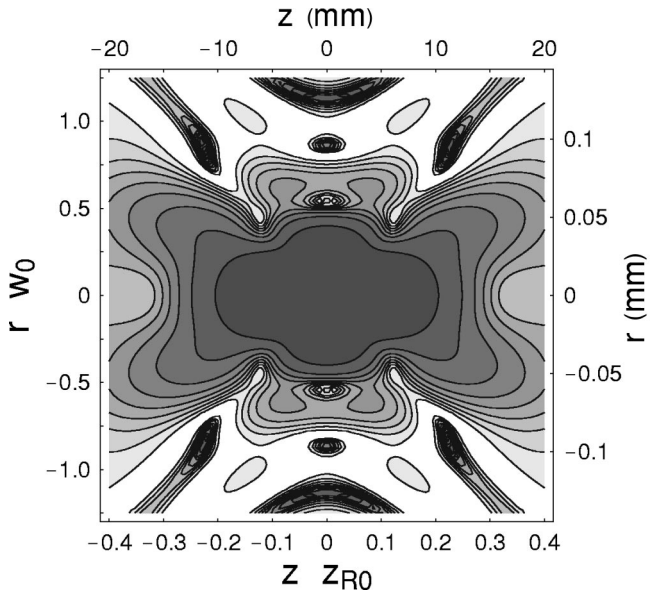

FIG. 3. Depth of modulation due to interference between forward and backward traveling beams. Black $=0$, white $=100\%$, and contours are at intervals of 10%.

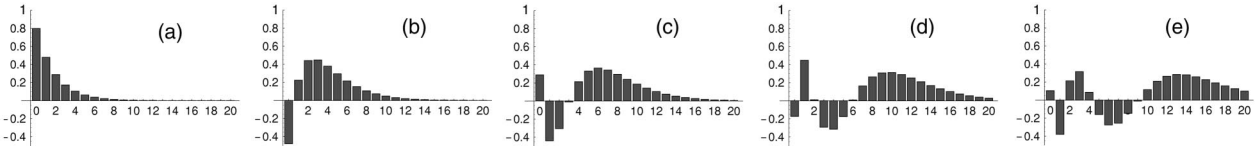

FIG. 4. Amplitudes of mode components corresponding to the (a) $\mathcal{L}_{00}$, (b) $\mathcal{L}_{10}$, (c) $\mathcal{L}_{20}$, (d) $\mathcal{L}_{30}$, and (e) $\mathcal{L}_{40}$ Laguerre-Gaussian beams for the case $\alpha=2$.

around 0.2 nm, we obtain a trap depth approaching 5 K. The col intensity is nearly half that at the center of a simple Gaussian beam of the same waist and total enhanced power, and almost twice that at the center of a TEM_{00} beam with the dimensions of the lowest-order cavity mode. In Fig. 2, we show—under high and low magnification—the optical field strength around the cavity center. For the larger-scale figure, we have averaged the field to remove structure on a wavelength scale, whose depth of modulation is shown in Fig. 3. This structure has a limiting value of $2/(a^6+a^{-6})=3\%$ at the dark trap center, while the col at the lowest part of the confining wall shows a value just below 4%. The values of the coefficients a_{p0q} are shown for $q=0$–4 in Figs. 4(a)–4(e), and their superposition a_{p0} in Fig. 5(a).

IV. IMPERFECT CAVITIES

Analysis in terms of Laguerre-Gaussian cavity modes allows the effect of finite mirror reflectivity and misadjustment to be determined. For a cavity of length $l'=l+\Delta l$, at a wavelength for which the lowest-order mode $\mathcal{L}_{00}^{(0)}$ is resonant, the Gouy shift per half round trip relative to that for a confocal cavity will be given by

$$\phi_{pm}=2(2p+|m|)\left\{\tan^{-1}\left(\frac{l'}{2z_R}\right)-\frac{\pi}{4}\right\}. \tag{17}$$

For mirror amplitude reflection and transmission coefficients $r_{1,2}$ and $t_{1,2}$, the forward and backward traveling fields of the circulating modes at the cavity center may be written in terms of the components of the incident beam as [30]

$$\mathcal{L}_{p0}^{+}(0,0)=\frac{t_1\exp \mathrm{i}\,\phi_{p0}/2}{1-r_1r_2\exp 2\mathrm{i}\,\phi_{p0}}a_{p0}\mathcal{L}_{p0}^{(0)}(0,0), \tag{18}$$

$$\mathcal{L}_{p0}^{-}(0,0)=\frac{t_1r_2\exp 3\,\mathrm{i}\,\phi_{p0}/2}{1-r_1r_2\exp 2\mathrm{i}\,\phi_{p0}}a_{p0}\mathcal{L}_{p0}^{(0)}(0,0). \tag{19}$$

Recalculating the mode superposition taking into account these complex transfer coefficients thus allows the field to be determined for an arbitrary mirror separation.

An optical cavity may be confocal only if the two mirrors have identical curvature or focal length, for the self-reproducing modes of each mirror—those which lie a focal length away and thus have Rayleigh lengths equal to the mirror focal lengths—must be identical. Should this not be the case, then an additional loss will be introduced corresponding to the incomplete projection of the mode of one mirror of focal length $f_a=(1+\delta/2)f_0$ (with waist radius $w_a=\sqrt{\lambda f_a/\pi}$) onto that of the other ($f_b=(1-\delta/2)f_0$, $w_b=\sqrt{\lambda f_b/\pi}$). The amplitude overlap o is given by Eqs. (8)–(12) with $p=0$ and $\alpha=w_a/w_b=\sqrt{f_a/f_b}$, yielding

$$o^2=1-(\delta/2)^2. \tag{20}$$

The difference in focal length is thus manifest as an effective reduction in the mirror reflectivity from R to $R[1-(\delta/2)^2]$. For $R=0.9999$, the effects of imperfect mode overlap and partial reflectivity will be equal when the focal lengths differ by 2%.

In Fig. 6, we show the intensity distribution around the center of a cavity whose 99.99% reflecting mirrors are 0.0001% (0.1 μm) from their confocal separation; the attenuation coefficients for the first 21 modes of the superposition are indicated in Fig. 5(b). The trapping field pattern is displaced axially (as we discuss in the following section) and shows a slight curvature that reflects the nonlinear increase in Gouy phase with mode number; the destructive interference that forms the dark trapping region is no longer exact, but the overall structure is qualitatively little changed. The

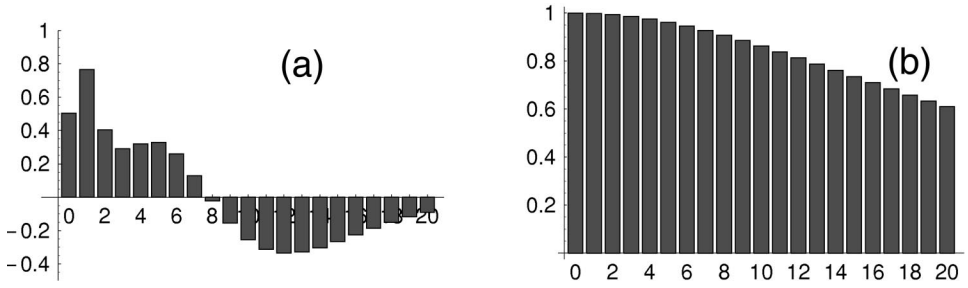

FIG. 5. (a) Amplitudes a_{p0} of mode components forming the complete five-component optical bottle beams, and (b) intensity attenuation coefficients for the optical bottle beam when the cavity mirrors are 0.1 μm from their confocal separation ($\Delta l/l=10^{-6}$), for $r^2=0.9999$, $t^2=0.0001$. 30 components were considered in calculating the subsequent field patterns.

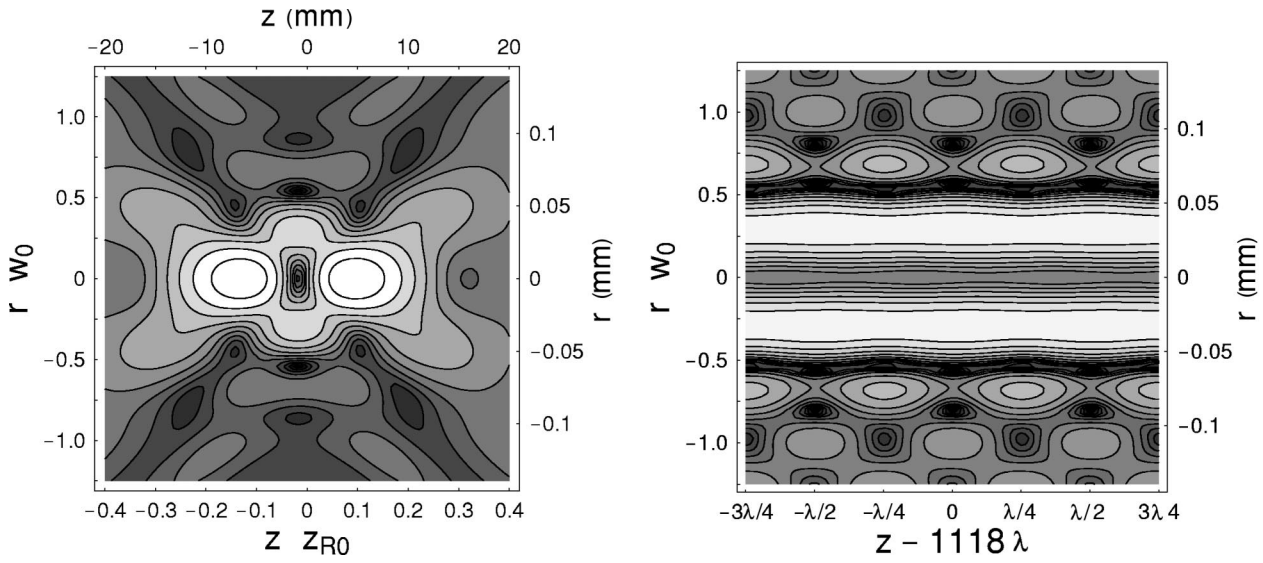

FIG. 6. Intensity distribution when the cavity mirrors are 0.1 μm from their confocal separation ($\Delta l/l = 10^{-6}$), for $r^2 = 0.9999$ and $t^2 = 0.0001$. The trap center lies 0.87 mm to the left of the cavity midpoint. Contours again refer logarithmically to the peak focal plane intensity in the ideal case.

modulation depth for the misaligned case is shown in Fig. 7; at the deepest part of the trap, the modulation is now around 13%, while at the col it has fallen slightly to around 3%.

The precision with which the mirror separation must be adjusted of course depends upon the resonator finesse, but with the laser wavelength locked to the lowest-order resonant mode, adjustment would be aided by observing the transmitted beam while the mirror spacing is varied. An image of the cavity center should show a smooth change in intensity, falling to zero as modes are brought into the superposition. The variation in intensity as a function of mirror displacement is shown for several radial positions in Fig. 8. The principal interpretation of this variation, as we shall discuss in the following section, is an amplified motion of the trap center as the mirror is displaced, suggesting that monitoring the trap position itself might be the best manner of adjustment.

We note that if the trapped species are sufficiently dense then the cavity field will itself be modified. This process, also analyzed in terms of nearly degenerate Laguerre-Gaussian modes, has recently been proposed as a means of tracking the motion of a particle contained within the cavity [31].

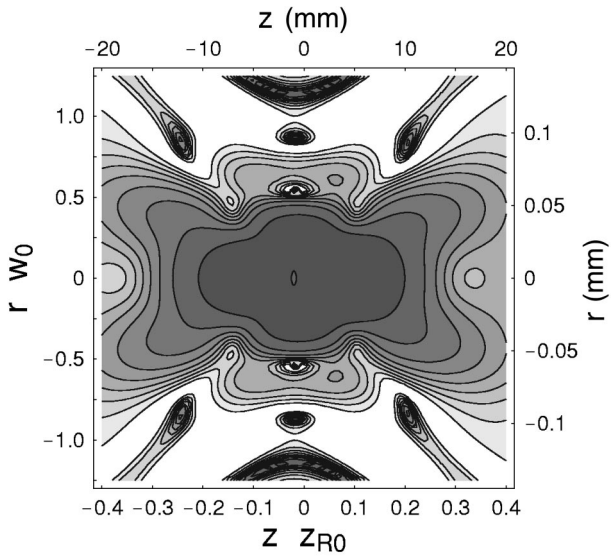

FIG. 7. Depth of modulation when the cavity mirrors are 0.1 μm from their confocal separation. Black = 0, white = 100%, contours are at 10% intervals.

V. A MECHANICAL AMPLIFIER

The magnitudes of the components $\mathcal{L}_{p0}^{\pm}(0,0)$ are maximum when the cavity is confocal and, therefore, vary only as second or higher-order powers of the mirror displacement from confocality. Since the cavity modes all have waists in

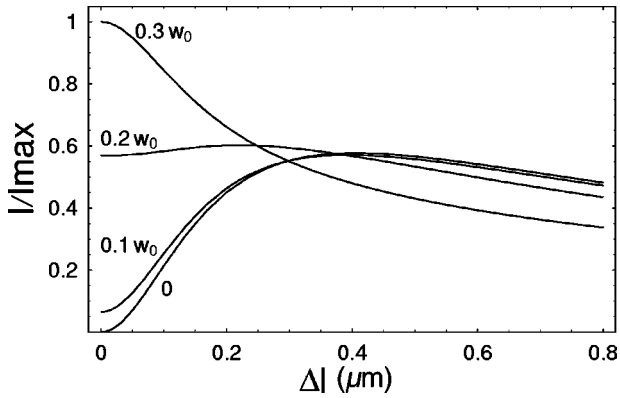

FIG. 8. Variation of focal plane intensity as cavity mirrors are displaced from their confocal separation, shown for points 0, 0.1 w_0, 0.2 w_0, and 0.3 w_0 from the cavity center and in units of the peak ideal focal plane intensity. The intensity in each case continues to fall monotonically at larger displacements. An image of the cavity center would serve during alignment of the cavity.

the focal plane, their radial dependence is also stationary around the trap center. For small mirror displacements around the confocal condition, the principal effect upon the mode superposition is thus via the component phases.

For each half round trip, the phase shift ϕ_{pm} can be rewritten (recalling that $z_R = l/2$) as

$$\phi_{pm} = 2(2p+|m|)\tan^{-1}\left(\frac{\Delta l/l}{2+\Delta l/l}\right) \approx 2(2p+|m|)\Delta l/l, \tag{21}$$

and thus varies linearly with Δl for small displacements. Its effect upon the component coefficients is to introduce a magnified phase,

$$\phi_{pm}^{(c)} = \arg\left(\frac{t_1 \exp \mathrm{i}\, \phi_{pm}/2}{1-r_1 r_2 \exp 2\mathrm{i}\, \phi_{pm}}\right) \tag{22}$$

$$= \frac{\phi_{pm}}{2} + \tan^{-1}\left(\frac{r_1 r_2 \sin 2\phi_{pm}}{1-r_1 r_2 \cos 2\phi_{pm}}\right) \tag{23}$$

$$\approx \phi_{pm}\left(\frac{1}{2} + \frac{2r_1 r_2}{1-r_1 r_2}\right) \tag{24}$$

$$\approx \frac{2\phi_{pm}}{1-r_1 r_2}, \tag{25}$$

where the approximations refer successively to ($|\phi_{pm}| \ll 1$) and ($r_1 r_2 \approx 1$).

These phase shifts will be canceled at a certain distance from the cavity center by the Gouy shift, which near the center is given approximately, and relative to that of the lowest-order mode, by

$$\phi_G \approx (2p+|m|)\frac{z}{z_R}. \tag{26}$$

The phase introduced by the mirror displacement is thus canceled when

$$(2p+|m|)\frac{z}{z_R} = \frac{2}{1-r_1 r_2}(2p+|m|)\frac{\Delta l}{l}, \tag{27}$$

which, again recalling that $z_R = l/2$, gives for all modes the common displacement

$$z = -\frac{\Delta l}{1-r_1 r_2}. \tag{28}$$

Small displacements of the mirrors from the confocal separation thus leave the form and dimensions of the trapping field largely unchanged, but are manifest as a magnified motion of the trap center. This is apparent from a comparison of Figs. 2 and 6: the trapping potentials are essentially similar, but the trap center is displaced by 0.87 mm as a result of the mirror displacement of 0.1 μm. The position and intensity of the trap center and the intensity of the confining col are shown as functions of the mirror displacement in Fig. 9.

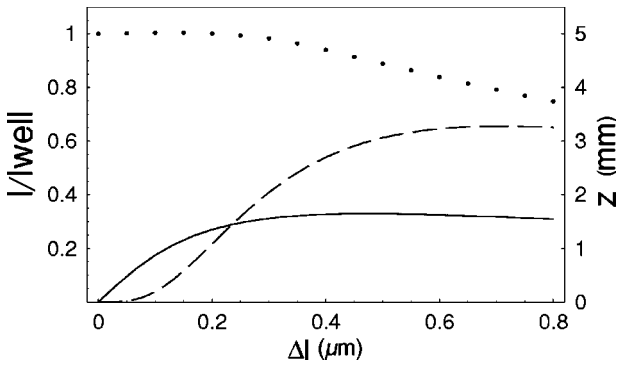

FIG. 9. Variation of trap col (dotted line) and trap center (dashed line) intensities—in units of the well depth at zero mirror displacement—and trap center position (solid line, right-hand scale) as cavity mirrors are displaced from their confocal separation.

As the phase shifts produced by small mirror movements are compensated only by the difference in Gouy phase between interfering cavity modes, the amplification mechanism may be compared to that of a Vernier scale. The effect may be regarded as occurring either between the five Laguerre-Gaussian components of the incident beam, or alternatively between the numerous cavity modes into which they are resolved. If an atom, molecule, or more macroscopic particle is trapped in the radiation field, then the cavity may be regarded as a high-gain mechanical amplifier.

The Vernier sensitivity to mirror displacement of traps formed by the interference of copropagating beams contrasts with the relative insensitivity of geometries in which the interfering beams counterpropagate, such as the array of dark coaxial rings that we have considered in a previous paper [27]. Fluctuations in the trap position can lead to heating of a trapped sample, and the use of this geometry as a cavity-enhanced dipole trap would thus require careful stabilization of the cavity mirror spacing. Fortunately, cavity locking techniques—that are essentially alternative methods of measuring the phase shift introduced by the mirror displacement—are highly developed and well understood. For best stability, the cavity could be locked to a reference laser of a second wavelength at which the finesse is rather higher than at the trapping wavelength. An alternative method would be to monitor the position of a trapped sample by observing sideways fluorescence using a small video camera.

It would be appropriate at this point to suggest situations in which this Vernier amplification could be a blessing rather than a curse, for there are few examples of mechanical amplifiers of this gain and sensitivity, but we are unfortunately unable to offer any serious proposals. Certainly the use of charge-coupled device arrays or even quadrant photodetectors would allow the position of a trapped object or sample to be determined with a precision corresponding to mirror displacements of the order of an atomic spacing, or to the presence within the cavity of tiny concentrations of a dispersive vapor, but then conventional cavity-locking techniques would do likewise. Trapped species such as hollow particles or ensembles of atoms or molecules could be moved macroscopic distances by merely controlling a piezoactuated mir-

ror mount; indeed, the recent use of optical tweezers to transport Bose-Einstein condensates [6] shows how dipole forces are of unique importance to studies of quantum degenerate gases.

VI. CONCLUSION

We have shown that optical bottle beams suitable for the dipole-force confinement of dark-field-seeking atoms and molecules may be enhanced by a confocal cavity that is simultaneously resonant for all the component modes. The Gouy phase introduces a difference—readily apparent using geometrical optics—between forward and backward traveling beams that eliminates the nodal planes of complete cancellation, along which the dark-field-seeking species would otherwise escape. For the example of a trap for atomic rubidium, we find that the powers typical of laser diodes may yield enhanced trap depths of several kelvin.

By adding further Laguerre-Gaussian components to the basic superposition, we have shown that it is possible to increase the depth of the bottle beam potential without changing the overall geometry. As an illustration, we have considered a five-component version of the optical bottle beam that, for the same laser power and similar beam radii, is 85% deeper than the simplest, two-component combination.

Finally, our analysis of the variation of the trapping field as the mirrors are displaced from their confocal separation shows an amplified displacement of the trap center from the center of the cavity, allowing the cavity-enhanced dipole-force trap to be used as a mechanical amplifier with a gain roughly equal to the intensity enhancement factor of the cavity.

ACKNOWLEDGMENTS

The authors are grateful for support from the European Commission and the U.K. Engineering and Physical Sciences Research Council in the course of this work.

[1] R. Grimm, M. Weidemüller, and Y.B. Ovchinnikov, Adv. At., Mol., Opt. Phys. **42**, 95 (2000).
[2] S.L. Rolston, C. Gerz, K. Helmerson, P.S. Jessen, P.D. Lett, W.D. Phillips, R.J. Spreeuw, and C.I. Westbrook, Proc. SPIE **1726**, 205 (1992).
[3] J.D. Miller, R.A. Cline, and D.J. Heinzen, Phys. Rev. A **47**, R4567 (1993).
[4] S. Chu, J.E. Bjorkholm, A. Ashkin, and A. Cable, Phys. Rev. Lett. **57**, 314 (1986).
[5] M.D. Barrett, J.A. Sauer, and M.S. Chapman, Phys. Rev. Lett. **87**, 010404 (2001).
[6] T.L. Gustavson, A.P. Chikkatur, A.E. Leanhardt, A. Gorlitz, S. Gupta, D.E. Pritchard, and W. Ketterle, Phys. Rev. Lett. **88**, 020401 (2002).
[7] S. Kuhr, W. Alt, D. Schrader, M. Müller, V. Gomer, and D. Meschede, Science **293**, 278 (2001).
[8] T. Takekoshi, B.M. Patterson, and R.J. Knize, Phys. Rev. Lett. **81**, 5105 (1998).
[9] R. Ozeri, L. Khaykovich, and N. Davidson, Phys. Rev. A **59**, R1750 (1999).
[10] N. Davidson, H.J. Lee, C.S. Adams, M. Kasevich, and S. Chu, Phys. Rev. Lett. **74**, 1311 (1995).
[11] P. Rudy, R. Ejnisman, A. Rahman, S. Lee, and N.P. Bigelow, Opt. Express **8**, 159 (2001).
[12] T. Kuga, Y. Torii, N. Shiokawa, T. Hirano, Y. Shimizu, and H. Sasada, Phys. Rev. Lett. **78**, 4713 (1997).
[13] S.A. Webster, G. Hechenblaikner, S.A. Hopkins, J. Arlt, and C.J. Foot, J. Phys. B **33**, 4149 (2000).
[14] R. Ozeri, L. Khaykovich, N. Friedman, and N. Davidson, J. Opt. Soc. Am. B **17**, 1113 (2000).
[15] Y.B. Ovchinnikov, I. Manek, A.I. Sidorov, G. Wasik, and R. Grimm, Europhys. Lett. **43**, 510 (1998).
[16] L. Cacciapuoti, M. de Angelis, G. Pierattini, and G.M. Tino, Eur. Phys. J. D **14**, 373 (2001).
[17] S. Kulin, S. Aubin, S. Christe, B. Peker, S.L. Rolston, and L.A. Orozco, J. Opt. B: Quantum Semiclassical Opt. **3**, 353 (2001).
[18] J. Arlt, K. Dholakia, L. Allen, and M.J. Padgett, J. Mod. Opt. **45**, 1231 (1998).
[19] J. Arlt and M.J. Padgett, Opt. Lett. **25**, 191 (2000).
[20] J. Ye, D.W. Vernooy, and H.J. Kimble, Phys. Rev. Lett. **83**, 4987 (1999).
[21] W.H. Pinkse, T. Fischer, P. Maunz, T. Puppe, and G. Rempe, J. Mod. Opt. **47**, 2769 (2000).
[22] A. Mosk, S. Jochim, H. Moritz, T. Elsässer, M. Weidemüller, and R. Grimm, Opt. Lett. **26**, 1837 (2001).
[23] J. Yin, Y. Zhu, W. Jhe, and Z. Wang, Phys. Rev. A **58**, 509 (1998).
[24] Y. Song, D. Milam, and W.T. Hill, Opt. Lett. **24**, 1805 (1999).
[25] X. Xu, V.G. Minogin, K. Lee, Y. Wang, and W. Jhe, Phys. Rev. A **60**, 4796 (1999).
[26] P. Zemánek and C.J. Foot, Opt. Commun. **146**, 119 (1998).
[27] T. Freegarde and K. Dholakia, Opt. Commun. **201**, 99 (2002).
[28] L. Allen, M.W. Beijersbergen, R.J.C. Spreeuw, and J.P. Woerdman, Phys. Rev. A **45**, 8185 (1992).
[29] J. Arlt, T. Hitomi, and K. Dholakia, Appl. Phys. B: Lasers Opt. **71**, 549 (2000).
[30] A. E. Siegman, *Lasers* (University Science Books, California, 1986), Sec. 11.3.
[31] P. Horak, H. Ritsch, T. Fischer, P. Maunz, T. Puppe, P.W.H. Pinkse, and G. Rempe, Phys. Rev. Lett. **88**, 043601 (2002).